Development 140, 3040-3050 (2013) doi:10.1242/dev.087858
© 2013. Published by The Company of Biologists Ltd

Zebrafish rhabdomyosarcoma reflects the developmental stage of oncogene expression during myogenesis

Narie Y. Storer[1,2], Richard M. White[3], Audrey Uong[1,2], Emily Price[1,2], G. Petur Nielsen[3], David M. Langenau[4] and Leonard I. Zon[1,2,*]

SUMMARY

Rhabdomyosarcoma is a pediatric malignancy thought to arise from the uncontrolled proliferation of myogenic cells. Here, we have generated models of rhabdomyosarcoma in the zebrafish by inducing oncogenic *KRAS^{G12D}* expression at different stages during muscle development. Several zebrafish promoters were used, including the *cdh15* and *rag2* promoters, which drive gene expression in early muscle progenitors, and the *mylz2* promoter, which is expressed in differentiating myoblasts. The tumors that developed differed in their ability to recapitulate normal myogenesis. *cdh15:KRAS^{G12D}* and *rag2:KRAS^{G12D}* fish developed tumors that displayed an inability to complete muscle differentiation as determined by histological appearance and gene expression analyses. By contrast, *mylz2:KRAS^{G12D}* tumors more closely resembled mature skeletal muscle and were most similar to well-differentiated human rhabdomyosarcoma in terms of gene expression. *mylz2:KRAS^{G12D}* fish showed significantly improved survival compared with *cdh15:KRAS^{G12D}* and *rag2:KRAS^{G12D}* fish. Tumor-propagating activity was enriched in *myf5*-expressing cell populations within all of the tumor types. Our results demonstrate that oncogenic *KRAS^{G12D}* expression at different stages during muscle development has profound effects on the ability of tumor cells to recapitulate normal myogenesis, altering the tumorigenic capability of these cells.

KEY WORDS: Rhabdomyosarcoma, Zebrafish, Muscle

INTRODUCTION

Rhabdomyosarcoma (RMS) is a pediatric malignancy thought to arise from the aberrant regulation of developmental programs during myogenesis. It is the most common soft-tissue sarcoma of childhood (Wexler and Helman, 1994; Arndt and Crist, 1999). Treatment approaches are often aggressive and multimodal, involving a combination of chemotherapeutic agents and local surgical resection and/or irradiation. Patients with locally unresectable or metastatic disease are particularly difficult to treat, and current treatment approaches have a considerable number of severe sequelae, including secondary malignancies (Wexler and Helman, 1994; Arndt and Crist, 1999). There is a need for novel therapies that specifically target the unique molecular underpinnings of this disease.

There are two major pediatric subtypes of RMS, embryonal (ERMS) and alveolar (ARMS), distinguished by histological appearance (Wexler and Helman, 1994; Arndt and Crist, 1999). ARMS is characterized in most cases by chromosomal translocations between the *PAX3* or *PAX7* and the *FKHR* (*FOXO1* – Human Gene Nomenclature Database) loci (Barr, 2001). By contrast, ERMS is often associated with loss of heterozygosity at chromosome 11p15 and a number of whole chromosomal gains (Wexler and Helman, 1994; Barr, 1997; Arndt and Crist, 1999). Activating mutations in RAS family members have been described in a minority of ERMS cases (Stratton et al., 1989; Chen et al., 2006; Martinelli et al., 2009), and gene expression analysis on a number of tumors suggests that RAS pathway activation might be a common event in ERMS formation, even in the absence of RAS mutations (Langenau et al., 2007).

The vast majority of skeletal muscle progenitors during vertebrate embryogenesis are derived from somites, epithelial condensations of the paraxial mesoderm that transiently form during anterior-posterior patterning of the embryo (Pownall et al., 2002; Parker et al., 2003). The myogenic regulatory factors (MRFs) MyoD (Myod1), Myf5, myogenin (also known as Myf4) and Myf6 (also known as Mrf4) are basic helix-loop-helix (bHLH) transcription factors that are important regulators of muscle development and differentiation. MyoD and Myf5 are expressed in early muscle progenitors within somites and together are required for and regulate muscle progenitor specification (Pownall et al., 2002). Myf6 and myogenin are expressed in more differentiated muscle cells and are the key regulators of muscle differentiation (Pownall et al., 2002). Postnatal muscle progenitors are thought to arise from satellite cells, the resident stem cells of adult skeletal muscle (Parker et al., 2003). The MRFs function similarly to their embryonic roles in directing the differentiation of satellite cell-derived progenitors into terminally differentiated muscle (Parker et al., 2003).

The myogenic program is disrupted in human RMS. RMS tumors consistently overexpress MYOD1, and variably express the other MRFs (Anderson et al., 1999; Blandford et al., 2006). They also express other myogenic factors that are characteristic of multiple stages of myogenesis and often express various structural proteins that are typically found in terminally differentiated muscle (Anderson et al., 1999; Blandford et al., 2006). Yet RMS tumors do not readily form myotubes and myofibers, suggesting an inability to activate myogenic programs appropriately (Anderson et al., 1999). Interestingly, expression of myogenin is correlated with disease progression and poor clinical outcome (Blandford et al., 2006; Heerema-McKenney et al., 2008), yet it is unclear whether it directly modulates disease phenotype or represents a marker of disease state in RMS.

[1]Stem Cell Program and Division of Hematology/Oncology, Boston Children's Hospital and Dana-Farber Cancer Institute, Boston, MA 02115, USA. [2]Harvard Medical School, Boston, MA 02115, USA. [3]Memorial Sloan-Kettering Cancer Center, New York, NY 10065, USA. [4]Massachusetts General Hospital, Boston, MA 02114, USA.

*Author for correspondence (zon@enders.tch.harvard.edu)

Accepted 7 May 2013

A handful of recent experiments have yielded insights into the tumor-initiating potential of a number of cell types during muscle development. In murine models, ARMS can develop from the introduction of PAX-FKHR into mesenchymal stem cells or Myf6-expressing terminally differentiating myofibers, but not in Pax7-expressing satellite cells (Keller et al., 2004b; Keller et al., 2004a; Ren et al., 2008). In another line of experiments, the introduction of T/t-Ag (SV40 large-T/small-T antigen), hTERT and H-Ras^{V12G} expression into committed adult human skeletal muscle myoblasts resulted in ERMS formation, whereas the introduction of the same genetic alterations into low-passage human fetal skeletal muscle precursor cells resulted in sarcomas lacking histopathological features of RMS (Linardic et al., 2005). Rubin and colleagues investigated the tumorigenic potential of multiple myogenic lineages using *Ptch1* and/or *p53* (*Trp53* – Mouse Genome Informatics) conditional mouse models (Rubin et al., 2011). Although a number of myogenic lineages were capable of giving rise to ERMS tumors, Myf6-expressing differentiating muscle cells had the highest propensity to form ERMS tumors, whereas Pax7-expressing satellite cells formed mostly undifferentiated sarcomas. In a study by Hettmer and colleagues, the introduction of *KrasG12V* and disruption of *CDKN2A;p16p19* in prospectively isolated satellite cells resulted in pleomorphic RMS formation; in a heterogeneous population of adipogenic and differentiating myogenic cells, these genetic changes led to tumors with varying levels of myogenic commitment (Hettmer et al., 2011). Finally, Hatley and colleagues demonstrated that murine ERMS can form when a conditionally active *Smo* allele is introduced into the adipocyte lineage (Hatley et al., 2012). Taken together, these data suggest that a number of cell types from myogenic and non-myogenic lineages harbor differing potentials to generate RMS. However, the pathways activated in these cell types that contribute to differing cell biology and myogenic differentiation remain to be uncovered.

In this study, we generated novel models of RMS in the zebrafish by inducing *KRAS^{G12D}* expression at different stages of muscle development using zebrafish *rag2*, *cdh15* and *mylz2* (*mylpfa* – Zebrafish Information Network) promoters. The models differed in their ability to recapitulate normal myogenesis, with *rag2* and *cdh15* tumors consisting of a large proportion of myoblast-like cells and *mylz2* tumors most closely resembling mature skeletal muscle. *rag2* and *cdh15* tumors were more aggressive than *mylz2* tumors and were more similar to less differentiated human RMS in terms of gene expression. We found that tumor-propagating activity was enriched in the least differentiated, *myf5*-expressing cell populations within the tumors, suggesting that a cellular hierarchy reminiscent of untransformed developing muscle cells exists within RMS tumors. This study highlights the importance of the developmental timing of oncogene expression on subsequent tumor formation and suggests that pathways regulating normal development can also have profound effects on tumor behavior.

MATERIALS AND METHODS

Zebrafish

Zebrafish were maintained and developmentally staged as previously described (Westerfield, 1989) and according to Institutional Animal Care and Use Committee guidelines. The Animal Care and Use Committee, Boston Children's Hospital, approved all animal protocols.

Vectors and cloning

cdh15 (4.1 kb) and *mylz2* (2.2 kb) promoter elements were PCR-amplified from wild-type AB strain genomic DNA (for all primer sequences, see supplementary material Table S3). Each forward primer contains a *Xho*I restriction digest site, and each reverse primer contains a *Bam*HI site. PCR products were purified, digested using *Xho*I and *Bam*HI, and cloned into the *rag2-GFP* vector (Langenau et al., 2003) to generate *cdh15:GFP* and *mylz2:GFP* vectors. These vectors were digested with *Bam*HI and *Hin*dIII to release the *GFP* cassette, and *KRAS^{G12D}* from the *rag2-KRAS^{G12D}* vector (Langenau et al., 2007) was inserted to generate *cdh15:KRAS^{G12D}* and *mylz2:KRAS^{G12D}* vectors. The generation of the *mylz2:mCherry* and *rag2-KRAS^{G12D}* constructs were previously described (Langenau et al., 2007; Smith et al., 2010).

Microinjection and transgenesis

The *cdh15:GFP*, *mylz2:mCherry*, *rag2:KRAS^{G12D}*, *cdh15:KRAS^{G12D}* and *mylz2:KRAS^{G12D}* vectors were linearized with *Xho*I, purified and diluted to 100 ng/μl in 0.5×TE + 0.1 M KCl. One nl of the *cdh15:GFP* and *mylz2:mCherry* vector dilutions were microinjected into one-cell-stage AB strain zebrafish embryos, and resulting F0 adult fish were incrossed to identify fluorescence-positive stable F1 transgenic fish. The F1 progeny were outcrossed to AB strain fish to propagate the lines. *mylz2:mCherry* fish were outcrossed to *myf5:GFP* (Chen et al., 2007) zebrafish to generate *myf5:GFP; mylz2:mCherry* double transgenic animals. The *rag2:KRAS^{G12D}*, *cdh15:KRAS^{G12D}* and *mylz2:KRAS^{G12D}* vector dilutions were microinjected into one-cell stage AB strain or *myf5:GFP; mylz2:mCherry* transgenic embryos to generate mosaic transgenic tumor-bearing fish.

Whole-mount RNA *in situ* hybridization

Segments (350-700 bp) of open reading frames for *GFP*, *mCherry*, *mylz2*, *cdh15*, *rag2* and *KRAS^{G12D}* genes were PCR amplified from the *rag2-GFP* or *cdh15:mCherry* vectors or from zebrafish tumor cDNA. Digoxigenin-labeled anti-sense and sense RNA probes were generated from purified PCR products using SP6 and T7 RNA polymerase, respectively, with the exception of the *KRAS^{G12D}* probes, which were generated using T7 and SP6 RNA polymerase, respectively. Whole-mount *in situ* hybridization on zebrafish embryos was performed as described (Thisse et al., 1993).

Histopathology

Fish were euthanized and fixed in 4% paraformaldehyde overnight at 4°C and decalcified in 0.5 M EDTA, pH 8. Paraffin embedding, sectioning, Hematoxylin and Eosin (H&E) staining and RNA *in situ* hybridization were performed according to standard techniques by the Brigham & Women's Pathology Core. RNA *in situ* probes used for staining of sections have been previously described (Langenau et al., 2007). For immunohistochemistry, paraffin-embedded sections were treated with xylene, rehydrated in a graded ethanol series, incubated in Citrate-based Antigen Unmasking Solution (Vector Laboratories) at 97°C for 20 minutes, and incubated in BLOXALL Blocking Solution (Vector Laboratories) for 10 minutes. Subsequent incubations were performed following the manufacturer's instructions using the Vectastain Elite ABC Kit (Vector Laboratories). Phospho-S6 Ribosomal Protein (Ser235/236) antibody (Cell Signaling #2211) was used at 1:400, and slides were counterstained with Hematoxylin.

Quantitative RT-PCR

RNA was isolated from whole tumor or normal muscle samples using TRIzol reagent (Invitrogen), treated with DNase I and purified using the RNeasy Mini Kit (Qiagen). cDNA synthesis was performed from equal amounts of RNA using SuperScript III First-Strand Synthesis SuperMix for qRT-PCR (Invitrogen), and quantitative RT-PCR was performed using SYBR GreenER qPCR SuperMix for iCycler (Invitrogen). Primer sequences used for QPCR are included in supplementary material Table S3. For each gene tested for every sample, relative gene expression was calculated from experimental triplicates by using the $2^{-\Delta\Delta CT}$ method (Livak and Schmittgen, 2001). For each experimental sample, ΔC_T was calculated by subtracting the C_T value for EF1a from the C_T value for the target gene. $\Delta\Delta C_T$ was then calculated by subtracting the ΔC_T for a single reference sample per gene from ΔC_T for the sample. Normalized relative gene expression was calculated using the $2^{-\Delta\Delta CT}$ formula and then averaged across experimental replicates, and gene transcript expression levels between tumor types were compared using Student's *t*-test.

Microarray analysis

RNA was isolated from seven tumors for each of the *rag2*, *cdh15* and *mylz2* tumor types and from seven normal zebrafish muscle samples using TRIzol reagent (Invitrogen). cDNA was prepared and hybridized to zebrafish Affymetrix arrays. Zebrafish data were analyzed using the Genepattern software suite (Broad Institute). Raw CEL files were converted into GCT format using the ExpressionFileCreator Module, with RMA and quantile normalization. The GCT file was then used in the PreprocessDataSet module, where threshold and ceiling values were set, and any value lower/higher than the threshold/ceiling were reset to the threshold/ceiling value, and data were processed to discard any invariant genes (genes with less than twofold change and mindelta 100). Comparisons between groups were performed using the ComparativeMarkerSelection modules, using two-sided *t*-test with Benjamini-Hochberg multiple hypothesis testing. Normalized, pre-processed data were used for unsupervised, hierarchical clustering via GenePattern. Row and column distance measurement was performed with the Pearson correlation, using pairwise complete-linkage, and both rows and columns were normalized. Microarray data have been deposited in Gene Expression Omnibus under accession number GSE39731.

Gene set enrichment analysis (GSEA)

The data from Davicioni et al. (Davicioni et al., 2009) were modified to stratify samples into survival of < or >2.5 years, or < or >5 years. Any sample without full survival data was censored, bringing the total number of usable samples from 186 to 156. Classifications (*.cls files) were made based on the conventions of Davicioni et al., including histological subtype, molecular subclass, and survival of 2.5 years or 5 years. This yielded a gct file containing the expression data of the 156 relevant human arrays, as well as several cls files used as the input to GSEA. Because the annotation between zebrafish and human datasets is necessarily imperfect, we converted the zebrafish Affymetrix probe IDs into the human Affymetrix U133A array probe ID, if possible. This then allowed for derivation of the human gene symbols (HUGO identifiers) for each relevant zebrafish comparison. GSEA was run using up- and downregulated HUGO gene lists from each zebrafish RMS type, querying against the various human RMS classes. Permutation number=1000, collapse dataset to symbols=true, and permutation type=gene_set as several subclassifications had fewer than seven samples. A false discovery rate (FDR) of <0.25 was considered a significant enrichment.

5-Ethynyl-2′-deoxyuridine (EdU) incorporation

Tumor-bearing fish were injected intraperitoneally with 10 µl of 2.5 mg/ml EdU per 0.25 g body weight. After 24 hours, fish were euthanized and frozen in Optimal Cutting Temperature medium at −80°C overnight. Cryostat sections (12 µm) were prepared, and EdU labeling was performed using the Click-iT EdU Alexa Fluor 594 Imaging Kit (Invitrogen). Labeled sections were imaged at 400× magnification using a compound fluorescent microscope, and the number of EdU-positive and DAPI-positive nuclei were counted in three separate 1.37×10^4 µm^2 fields per tumor. The ratios of EdU-positive to DAPI-positive nuclei in the three fields were averaged to calculate an EdU/DAPI ratio for each tumor.

Sample preparation and fluorescence-activated cell sorting (FACS)

Blood cells from AB strain fish, muscle cells from *mylz2:mCherry* fish, and tumor cells from *KRAS*^{G12D}-injected fish were isolated. Blood cells were re-suspended in 10 ml 0.9× PBS. Muscle and tumor cells were mechanically disrupted in 10 ml 0.9× PBS and incubated with 125 µl 2.5 mg/ml (13 WU/ml) Liberase TM enzyme blend (Roche) at room temperature for 30 minutes. Heat-inactivated FBS (500 µl) was added to each cell preparation, and samples were then filtered (40-µm cell strainer) and centrifuged at 1000 ***g*** for 5 minutes. Muscle and tumor cell suspensions were re-suspended in 1 ml 0.9× PBS + 2 mM $MgCl_2$ and incubated with 10 µl of 10 U/µl benzonase (Sigma) for 15-30 minutes at room temperature. To this, 9 ml of 0.9× PBS + 5% fetal bovine serum (FBS) was added, and samples were centrifuged at 1000 ***g*** for 5 minutes, re-suspended in 0.9× PBS + 5% FBS + 200 ng/ml DAPI, and re-filtered (40-µm cell strainer). FACS was performed as described (Traver et al., 2003; Langenau et al., 2007) on a BD FACSAria II Cell Sorter. Doublets were excluded by size, and dead cells were excluded by DAPI incorporation. For all samples, test sorts were performed to measure the purity of sorted populations.

Transplantation

Transplantation of tumor cells was performed as described (Langenau et al., 2007). Sorted cell populations were transplanted into irradiated *casper* fish (White et al., 2008) (10 Gy for primary transplantation, 20 Gy for secondary transplantation, 2 days prior to transplantation). Red blood cells were used as carrier cells for a total of 2×10^4 cells per transplantation. To assess for tumor engraftment, recipients were scored for GFP and mCherry fluorescence under a fluorescence dissecting microscope at 8 and 15 days post-transplantation. Fish with GFP- and/or mCherry-positive tumor masses were defined as having positive engraftment, and a subset of these fish was sectioned to verify engraftment by histology.

RESULTS

cdh15 and *mylz2* promoter elements drive gene expression in the developing musculature

5′ upstream promoter elements of the *cdh15* (*cadherin 15, M-cadherin*) and *mylz2* (*myosin light chain, phosphorylatable, fast skeletal muscle a*) genes were cloned from wild-type zebrafish

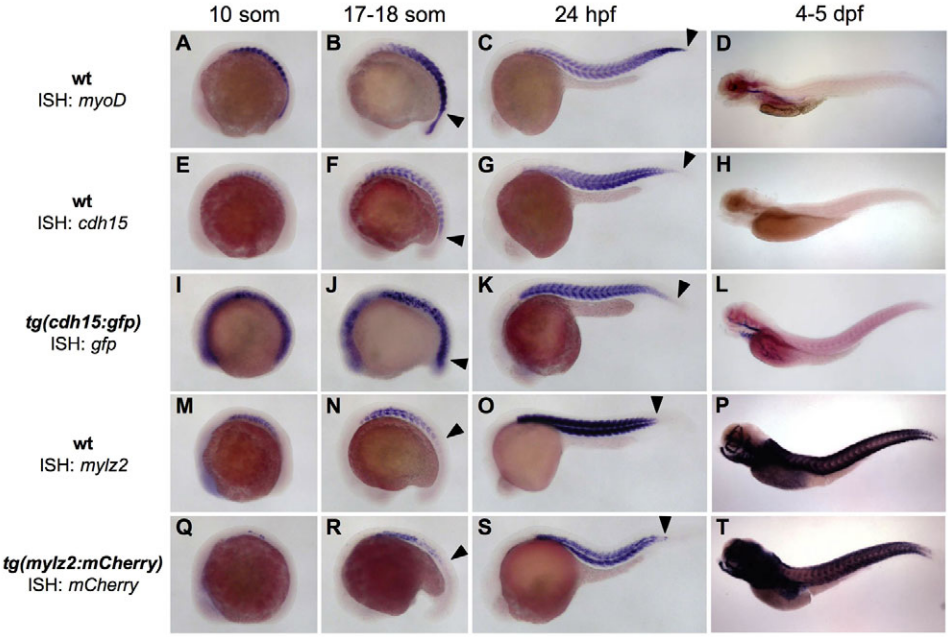

Fig. 1. *cdh15* and *mylz2* transgenic muscle promoters recapitulate endogenous expression patterns during development and turn on at different times during somite formation. Whole-mount RNA *in situ* hybridization was performed on endogenous genes in AB strain wild-type embryos (**A-H**,**M-P**), or the *GFP* (**I-L**) or *mCherry* (**Q-T**) transcript in transgenic embryos. dpf, days post-fertilization; hpf, hours post-fertilization; som, somite stage. Anterior is on the left. Arrowheads denote the location of the most posteriorly stained somite.

DEVELOPMENT

genomic DNA. *cdh15* is a marker of satellite cells and is also expressed in differentiating myoblasts where it contributes to myoblast fusion (Irintchev et al., 1994; Zeschnigk et al., 1995), whereas *mylz2* is a marker of more differentiated muscle in zebrafish (Xu et al., 2000). The *cdh15* and *mylz2* promoters were cloned into *GFP* and *mCherry* expression vectors, respectively, and injected into AB strain zebrafish embryos at the one-cell stage. The resulting transgenic animals displayed fluorophore expression throughout the musculature beginning at 1 day post-fertilization (dpf) for *cdh15:GFP* embryos, and 2 dpf for *mylz2:mCherry* embryos (data not shown). By RNA *in situ* hybridization, the *cdh15* and *mylz2* promoters were shown to drive gene expression similarly to their respective endogenous genes during development (Fig. 1E-T). *myoD* (*myod1* – Zebrafish Information Network) is expressed in the most newly formed somites of developing embryos (Fig. 1A-D), reflecting its early role in the specification of muscle progenitors. *GFP* transcript can be detected in nascent somites of *cdh15:GFP* embryos (Fig. 1I-K; supplementary material Fig. S1). By contrast, *mCherry* transcript is consistently found only in older and more anterior somites of *mylz2:mCherry* embryos during somitogenesis (Fig. 1Q-S). In addition, whereas *mCherry* transcript can be seen at high levels throughout the developed musculature of 5 dpf larvae, *GFP* transcript is barely detectable in the trunk musculature at 5 dpf (Fig. 1H,L,P,T). Gene expression analyses from adult fish also suggest that mCherry-positive cells from *mylz2:mCherry* fish express markers of muscle differentiation at higher levels than do GFP-positive cells from *cdh15:GFP* fish (supplementary material Fig. S2). Although both promoters drive gene expression in the muscle of developing zebrafish, the *cdh15* promoter drives expression earlier during myogenesis than the *mylz2* promoter.

KRAS^{G12D} expression driven by *rag2* and *cdh15* promoters results in RMS tumors that are less differentiated than *mylz2* tumors

A 6.9-kb zebrafish *rag2* promoter drives gene expression at low levels in the mononuclear compartment of the skeletal musculature (Langenau et al., 2007) that are undetectable by *in situ* hybridization of 5 dpf larvae (supplementary material Fig. S3) but can occasionally be seen in mononuclear cells of older larvae and adult fish (Langenau et al., 2007). Injection of a *rag2:KRAS^{G12D}* construct, containing human oncogenic *KRAS^{G12D}*, into zebrafish embryos results in the formation of RMS tumors (Langenau et al., 2007). To investigate further the effects of *KRAS^{G12D}* expression in the musculature, *rag2:KRAS^{G12D}*, *cdh15:KRAS^{G12D}* and *mylz2:KRAS^{G12D}* transgenic constructs were individually injected into AB strain zebrafish embryos at the one-cell stage. The resulting embryos express the *KRAS^{G12D}* transgene in a mosaic pattern consistent with endogenous expression patterns of the respective muscle promoters (supplementary material Fig. S4). In older larvae (5 dpf), *KRAS^{G12D}* expression can be detected in the musculature for all of the constructs. The mosaic transgenic zebrafish developed tumors that differed in histological appearance (Fig. 2A-G). Like *rag2* tumors, *cdh15* tumors comprise a heterogeneous population of spindle-shaped cells resembling myoblasts, multinucleated myofibers, and blood cells, consistent with classification as the spindle cell variant of ERMS. By contrast, *mylz2* tumors are relatively hypocellular, more closely resemble mature skeletal muscle, and contain a number of large, vacuolated cells (Fig. 2D-G). Tumors from the different models were assigned a differentiation score in a blinded fashion based on histological characteristics, including degree of cellularity and how closely tumors resemble

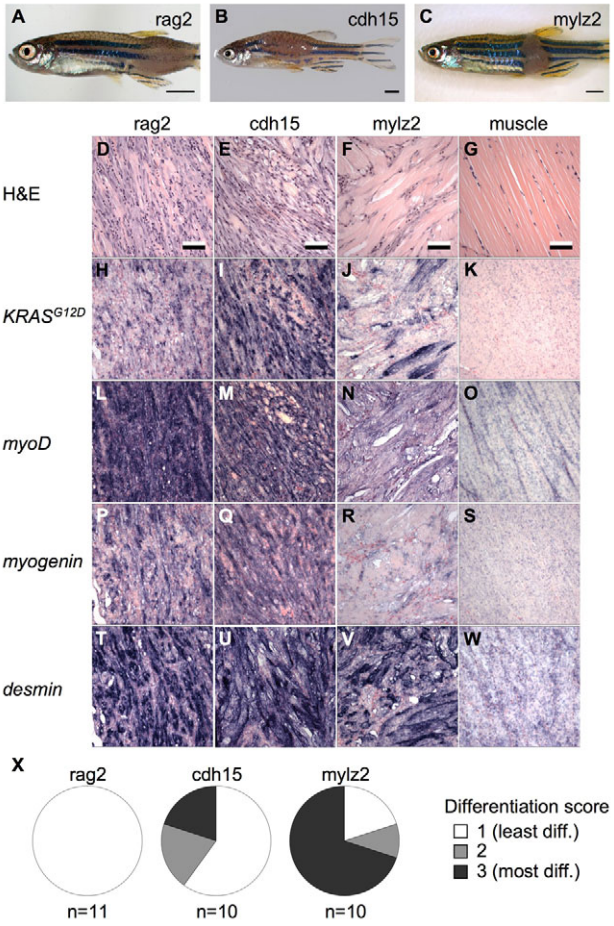

Fig. 2. Zebrafish injected with *rag2:KRAS^{G12D}*, *cdh15:KRAS^{G12D}* or *mylz2:KRAS^{G12D}* develop muscle tumors that differ in histological appearance. (**A-C**) Brightfield images of fish bearing *rag2* (A), *cdh15* (B) and *mylz2* (C) tumors. (**D-G**) H&E staining of tumors. (**H-W**) Tumors express diagnostic markers of RMS as assessed by RNA *in situ* hybridization. Histological sections of representative *rag2* (D,H,L,P,T), *cdh15* (E,I,M,Q,U) and *mylz2* (F,J,N,R,V) tumors and normal muscle (G,K,O,S,W). Images in D-W are at the same magnification. (**X**) Tumors were assigned differentiation scores based on histological appearance. Scale bars: in A-C, 2 mm; in D-G, 50 μm.

mature skeletal muscle. Overall, *rag2* and *cdh15* tumors appear less differentiated than *mylz2* tumors by histology (Fig. 2X).

Like *rag2* tumors, *cdh15* and *mylz2* tumors express *myoD*, *myogenin* and *desmin*, clinical diagnostic markers of RMS (Fig. 2L-W). Whereas a large proportion of cells in *rag2* and *cdh15* tumors display *myoD* and *myogenin* expression, only a small fraction express these markers in *mylz2* tumors. By quantitative RT-PCR, the *rag2* and *cdh15* tumors express the activated satellite cell markers *myf5* and *cdh15*, but not the quiescent satellite cell marker *pax7*, at significantly higher levels compared with the *mylz2* tumors (Fig. 3A-C; $P<0.05$). *rag2* tumors express higher levels of the myoblast differentiation gene *myogenin* compared with *mylz2* tumors (Fig. 3D; $P<0.05$). *rag2* tumors also express lower levels of *desmin*, which encodes an intermediate filament found in differentiated muscle (Fig. 3E; $P<0.05$). No difference was seen in levels of *mylz2* expression across the tumors (Fig. 3F; $P>0.05$). There was a detectable level of *KRAS^{G12D}* expression in *rag2* tumors. Although *KRAS^{G12D}* transcript levels appear higher in *cdh15* and *mylz2* tumors compared with *rag2* tumors, this difference

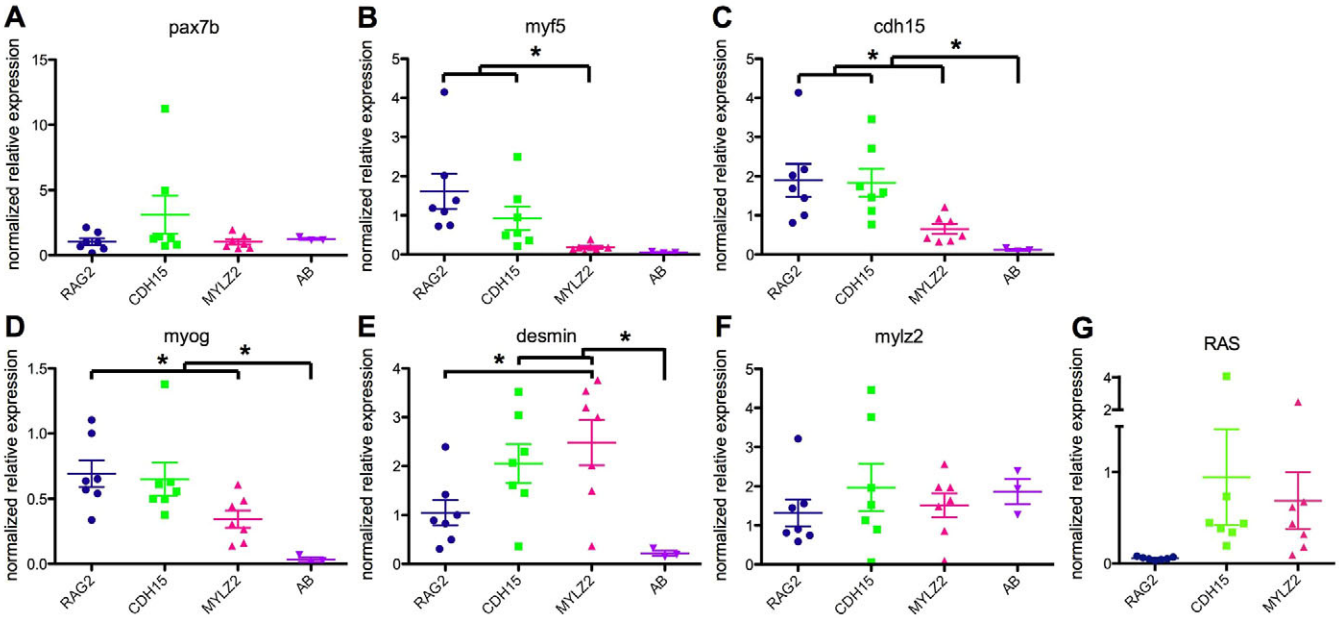

Fig. 3. *rag2:KRAS^{G12D}*, *cdh15:KRAS^{G12D}* and *mylz2:KRAS^{G12D}* tumors express myogenic markers at differing levels. Gene expression levels as determined by quantitative RT-PCR for the *pax7b* (**A**), *myf5* (**B**), *cdh15* (**C**), *myog* (**D**), *desmin* (**E**) and *mylz2* (**F**) genes or the *KRAS* (**G**) transgene. Asterisks indicate statistically significant differences between groups (P<0.05, Student's t-test). n=7 for each of the tumor models, and n=3 for normal muscle (AB strain). Error bars represent s.e.m.

was not statistically significant (Fig. 3G; P>0.05). Phospho-S6 ribosomal protein (pS6RP) levels, indicative of active RAS signaling, were similar among tumor types by immunohistochemistry (supplementary material Fig. S5). *rag2* and *cdh15* tumors express early and intermediate markers of myogenesis at higher levels than do *mylz2* tumors, reflecting a greater number of primitive myoblast-like cells in those tumors.

Survival of RMS tumor-bearing zebrafish varies among the tumor models

rag2 and *cdh15* tumors behave more aggressively than *mylz2* tumors. *mylz2* tumors develop with lower incidence compared with the *rag2* and *cdh15* models (*mylz2*, n=19 of 117; *rag2*, n=50 of 144; *cdh15*, n=42 of 146) and with longer latency (Fig. 4A; *rag2* versus *mylz2*, P=0.0004; *cdh15* versus *mylz2*, P<0.0001; *rag2* versus *cdh15*, P=0.73; log-rank test). *mylz2* tumor-bearing fish display increased survival over time compared with those bearing *rag2* or *cdh15* tumors (Fig. 4B; *rag2* versus *mylz2*, P=0.001; *cdh15* versus *mylz2*, P=0.009; *rag2* versus *cdh15*, P=0.72; log-rank test); median survival times were 63 days for *rag2* tumors, 46 days for *cdh15* tumors and 156 days for *mylz2* tumors. By histology, *mylz2* tumors generally appear more circumscribed and less invasive compared with the other tumor types (data not shown). The rate of EdU incorporation per total nuclei within the tumors over a 24-hour time period is not significantly different (Fig. 4C-L; P>0.05), and TUNEL staining within the tumors does not differ (data not shown). The differences in survival observed in the tumor types correspond to varying abilities to undergo muscle differentiation but do not correlate with measurable differences in the rate of proliferation or apoptosis.

Zebrafish RMS subtypes recapitulate the gene expression signatures of human RMS

Given the histological and phenotypic variation among the tumor types, we investigated whether this was reflected by differences in gene expression. We performed gene expression analysis using microarrays for each of the three subtypes of zebrafish RMS, along with normal muscle samples as controls. Unsupervised clustering revealed distinct clusters for the wild-type muscle and *mylz2* tumors, whereas the *rag2* and *cdh15* tumors were closer to each other (Fig. 5A), similar to what was seen at the histological level. This indicates that each of these tumor types harbor distinct molecular signatures. To quantify this on a global level, the up- and downregulated genes for each tumor type were generated by comparing array data for each of the tumor types to normal muscle (greater than twofold change, FDR<0.05) as shown in Fig. 5B and supplementary material Table S1. Across the three tumor types, we found that 664 genes were dysregulated (compared with normal muscle), demonstrating considerable molecular overlap between these histologically distinct tumors. However, as suggested by clustering, the *rag2* and *cdh15* tumors appear much more similar to each other than to the *mylz2* tumors: 208 genes (96 upregulated, 112 downregulated) were shared between the *rag2* and *cdh15* tumors, whereas the *mylz2* tumors only shared 56 genes (30 upregulated, 26 downregulated) with the *rag2* tumors. The *mylz2* tumors exhibited upregulation of genes more reminiscent of normal muscle, such as *troponin* (*tnnt3a*) and *myosin light peptide 7* (*myl7*), and had significantly higher levels of genes such as *tropomyosin 1* (*tpm1*) than did the *rag2* and *cdh15* tumors. This suggests that at the molecular level, consistent with the histological analysis, the *mylz2* tumors appear to be more differentiated than the *rag2* or *chd15* tumors.

To understand whether these zebrafish gene signatures correspond to the molecular changes found in human RMS, we compared the zebrafish tumor signatures with a large collection of annotated human RMS tumors using GSEA (Davicioni et al., 2009). We utilized the histological and molecular classification scheme in the Davicioni analysis, and considered the 156 human tumors that had complete annotation. This allowed for a classification of the human tumors into well-differentiated (WD), moderately differentiated (MD) and undifferentiated (UDS) subtypes. Genes

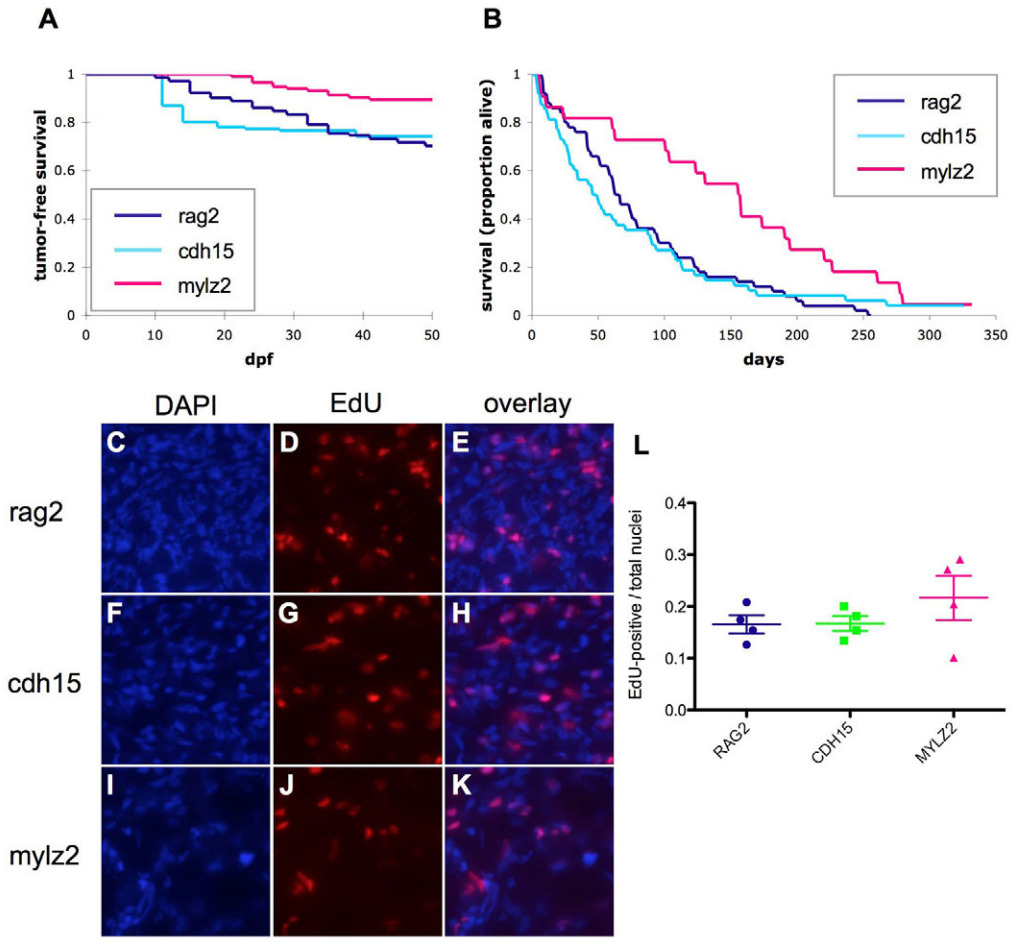

Fig. 4. Survival of tumor-bearing fish differs in *rag2*, *cdh15* and *mylz2* tumors. (**A**) Fish injected with *rag2:KRAS*^{G12D}, *cdh15:KRAS*^{G12D} or *mylz2:KRAS*^{G12D} transgenes developed tumors with differing latency and incidence (*mylz2*, *n*=19/117; *rag2*, *n*=50/144; *cdh15*, *n*=42/146 fish developed tumors; *rag2* versus *mylz2*, *P*=0.0004; *cdh15* versus *mylz2*, *P*<0.0001; *rag2* versus *cdh15*, *P*=0.73). (**B**) *mylz2* tumor-bearing fish displayed better survival over time compared with *rag2* and *cdh15* tumor-bearing fish (*rag2*, *n*=50; *cdh15*, *n*=48; *mylz2*, *n*=22; *rag2* versus *mylz2*, *P*=0.001; *cdh15* versus *mylz2*, *P*=0.009; *rag2* versus *cdh15*, *P*=0.72). *P*-values for A and B were calculated using the log-rank test. (**C-L**) Rates of EdU incorporation did not significantly differ among the tumor models. Fluorescent microscopic images depicting DAPI-positive (C,F,I) and EdU-positive (D,G,J) nuclei. (E,H,K) Merged images. (C-E) *rag2* tumor. (F-H) *cdh15* tumor. (I-K) *mylz2* tumor. (L) Quantification of the ratio of EdU-positive to total nuclei. *n*=4 for each tumor model; *P*>0.05, Student's *t*-test. Ratios were calculated based on the average ratio for three separate high-power images per tumor. Error bars represent s.e.m.

upregulated in the *mylz2* tumors (compared with the *rag2* or *cdh15* tumors) were enriched in the human WD tumors [*mylz2* versus *rag2*: normalized enrichment score (NES)=2.06, family-wise error rate (FWER)=0.00, FDR=0.00; *mylz2* versus *cdh15*: NES=1.88, FWER=0.001, FDR=0.001], consistent with the observation that the zebrafish *mylz2* tumors are the most well-differentiated (Fig. 5C,D; supplementary material Table S1). Similarly, genes upregulated in the *rag2* tumors were enriched in the human UDS tumors (*rag2* versus *cdh15*: NES=1.50, FWER=0.112, FDR=0.089) compared with human MD tumors, indicating that the *rag2* tumors are most similar to human undifferentiated rhabdomyosarcoma (data not shown).

To understand which classes of genes are most affected in each tumor subtype, the genes characterizing each subtype were analyzed using Ingenuity Pathway Analysis. The *mylz2* and *rag2* tumors were most easily differentiated by genes that play roles in glycolysis (e.g. *pgm1*, *hk1*, *aldoa*, upregulated in the *mylz2* versus *rag2* tumors) as well as the phosphatase and tensin homolog (PTEN) signaling pathway (e.g. *fgfr3*, *fgfr4*, *ccnd1*, *rac3*, *magi*), suggesting that alterations in metabolism might underlie differences in tumor subtypes. Taken together, these data indicate that the histological observation of differentiation status in the zebrafish tumors recapitulates the molecular distinctions of human RMS differentiation.

myf5-expressing cells are enriched for tumor-propagating activity in all zebrafish RMS subtypes

Previous experiments have shown that fluorescently labeled cell populations of *rag2* tumors generated in *myf5:GFP; mylz2:mCherry* double transgenic zebrafish are molecularly distinct and represent cells at differing stages of muscle differentiation (Ignatius et al., 2012). Moreover, in this background, *myf5:GFP*-positive/*mylz2:Cherry*- negative cells in *rag2* tumors, representing the least differentiated cell types, were highly enriched for tumor-propagating activity (Ignatius et al., 2012). In order to determine whether similar cell populations are enriched for tumor-propagating activity in the other RMS types, *rag2:KRAS*^{G12D}, *cdh15:KRAS*^{G12D} or *mylz2:KRAS*^{G12D} constructs were injected into one-cell-stage *myf5:GFP; mylz2:mCherry* zebrafish embryos (Fig. 6). When observed grossly, all tumors in this transgenic background display

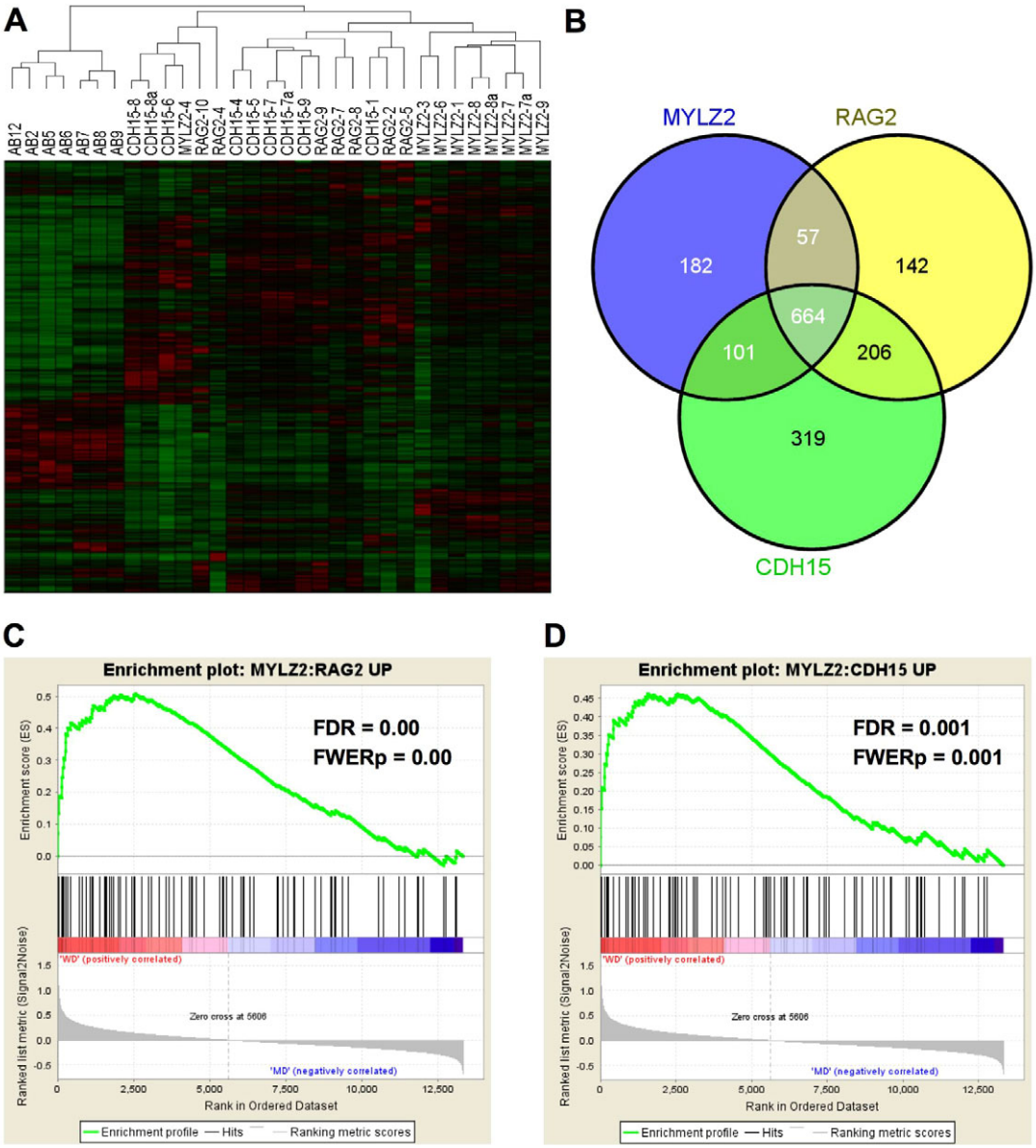

Fig. 5. Microarray analysis of zebrafish RMS driven by the *rag2*, *cdh15* or *mylz2* promoters. (**A**) Unsupervised hierarchical clustering of wild-type muscle (AB strain) or each of the three zebrafish RMS subtypes. The *mylz2* tumors are transcriptionally the most distinct, whereas the *rag2* and *cdh15* tumors are more similar to each other. (**B**) Venn diagrams showing overlap of dysregulated genes in each RMS subtype. Each tumor was compared with wild-type muscle, and gene numbers represent the sum of both up- and downregulated genes. For breakdown of up- and downregulated genes separately, see supplementary material Table S1. (**C**,**D**) GSEA plots showing enrichment of the *mylz2* signature (compared with *rag2* or *cdh15*) in human well-differentiated (WD) RMS. For expanded GSEA analysis, see supplementary material Table S1.

high levels of mCherry expression (Fig. 6C,F,I,L). Whereas *rag2* and *cdh15* tumors brightly express GFP, *mylz2* tumors appear either extremely dim or grossly negative for GFP fluorescence (Fig. 6B,E,H,K). FACS analysis on the mononuclear component of the tumors confirmed that only a small fraction of cells in the *mylz2* tumors are dimly GFP-positive compared with *rag2* and *cdh15* tumors (Fig. 7).

Tumors were then FACS-sorted based on GFP (G) and mCherry (R) positivity into G+R–, G+R+, G–R+ and G–R– populations (Fig. 7B-E,G-J,L-O). In the examples depicted in Fig. 7, the purity of cell populations were: for the *rag2* tumor, G+R– 92.0%, G+R+ 91.4%, G–R+ 73.7%, G–R– 99.8%; for the *cdh15* tumor, G+R– 93.1%, G+R+ 80.9%, G–R+ 73.6%, G–R– 99.8%; and for the *mylz2* tumor, G+R– 92.1%, G+R+ 94.9%, G–R+ 89.0%, G–R– 100.0%. Sorted cell populations were transplanted into irradiated *casper* recipients at limiting dilution (1×10^4, 1×10^3, 100 and ten cells). *casper* strain zebrafish are almost entirely transparent as adults, allowing for the rapid detection of transplanted tumor cells (White et al., 2008). Interestingly, the G+R– and G+R+ populations were enriched for engraftment potential in irradiated recipients compared with G–R+ and G–R– populations for each of the tumor models (Table 1; n=2 for each tumor type). For example, when 1000 G+R–, G+R+ or G–R+ cells were transplanted, engraftment was seen, respectively, in: 8/10, 7/10 and 0/10 fish for the *rag2* tumor; 4/8, 2/8 and 0/8 fish for the *cdh15* tumor; and 6/6, 8/10 and 1/9 fish for the *mylz2* tumor. *rag2* and *cdh15* engrafted tumors were consistently

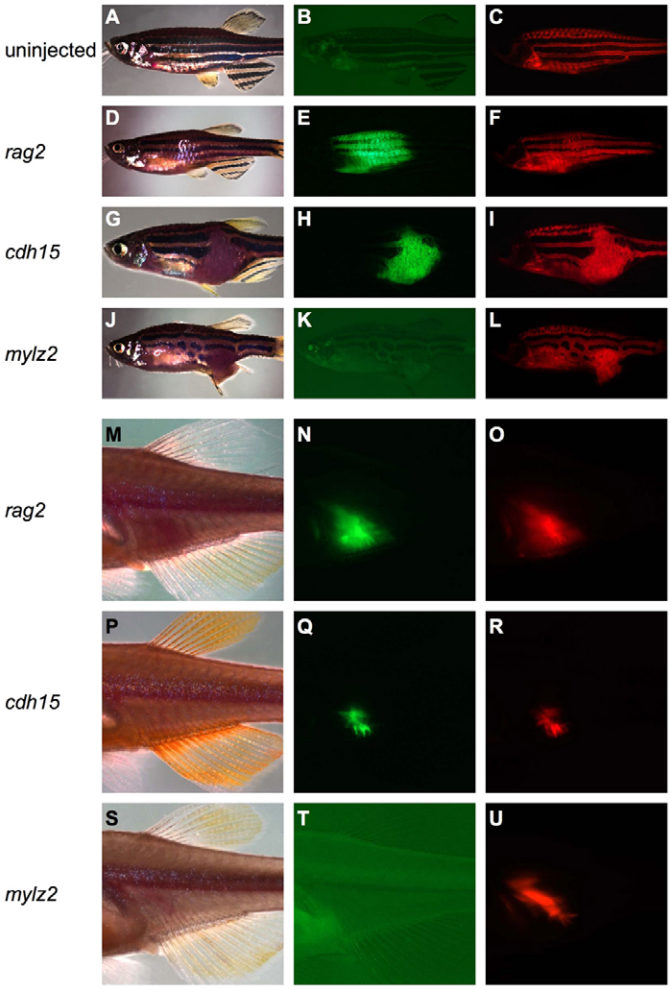

Fig. 6. Tumors in the *myf5:GFP;mylz2:mCherry* background differ in the degree of GFP fluorescence. (**A-L**) Brightfield (A,D,G,J), GFP (B,E,H,K) and mCherry (C,F,I,L) fluorescent images of uninjected fish (A-C) or tumor-bearing fish that had been injected with the *rag2:KRAS*^{G12D} (D-F), *cdh15:KRAS*^{G12D} (G-I) or *mylz2:KRAS*^{G12D} (J-L) transgenes at the one-cell stage. (**M-U**) Engrafted, secondary tumors in irradiated *casper* recipient fish display similar patterns of fluorescence to their respective primary, parent tumors. Brightfield (M,P,S), GFP fluorescence (N,Q,T), and mCherry fluorescence (O,R,U) images of *casper* fish transplanted with G+R– cells from a *rag2* tumor (M-O), *cdh15* tumor (P-R) or *mylz2* tumor (S-U).

larger than *mylz2* tumors (data not shown). Whereas the G–R+ population of *rag2* and *cdh15* tumors exhibited no engraftment potential at 1×10^4 cells, the G–R+ population of *mylz2* tumors was able to engraft when as few as 100 cells were transplanted. When G+R– cells were transplanted into *casper* recipients, the engrafted tumors that developed closely resembled the parent tumor by fluorophore expression for each of the tumor models (Fig. 6M-U). G+R– cells from *rag2* and *cdh15* tumors yielded engrafted tumors that were positive for both GFP and mCherry expression, whereas dim G+R– cells from *mylz2* tumors yielded tumors that were mCherry-positive, but only dimly GFP-positive or GFP-negative as observed grossly.

To confirm the engraftment potential of GFP-expressing cells, engrafted tumor cells from *rag2* and *cdh15* G+R– primary transplants were FACS sorted and found to contain G+R–, G+R+, G–R+ and G–R– cell populations. Sorted cells were transplanted into secondary irradiated recipients at limiting dilution (10^3, 100 and ten cells). As in the primary recipients, the G+R– and G+R+ populations of *rag2* and *cdh15* engrafted tumors were enriched for tumor-propagating activity, with as few as ten GFP-positive cells required for engraftment (supplementary material Table S2). As previously reported (Ignatius et al., 2012), G+R– cells from the *rag2* tumors exhibited a significant enrichment for long-term, serial engraftment potential compared with either the G+R+ or G–R+ cell subpopulations (P=0.034, limdil software). Secondary transplantation of *mylz2* tumors could not be completed owing to the low number of engrafted cells within primary recipients. From these transplantation experiments, we conclude that the *myf5:GFP*-expressing subpopulation within *rag2*, *cdh15* and *mylz2* tumors is enriched for tumor-propagating activity.

DISCUSSION

Dysregulation of myogenesis in RMS

Clinical RMS is characterized by the inability to undergo normal muscle differentiation, despite the overexpression of MRFs in tumors (Anderson et al., 1999; Blandford et al., 2006). The mechanisms underlying this block in myogenesis and the importance of dysregulation of myogenic programs in RMS are largely unknown. In this study, zebrafish RAS-induced RMS displayed varying capabilities to implement the myogenic program. *rag2* and *cdh15* tumors had a large number of primitive, myoblast-like cells with inefficient myotube and myofiber formation, reminiscent of the spindle cell variant of ERMS, whereas *mylz2* tumors more closely resembled mature skeletal muscle. This difference was reflected at the gene expression level; *rag2* and *cdh15* tumors expressed higher levels of the satellite cell and early myoblast markers *myf5* and *cdh15*, and *mylz2* tumors preferentially expressed structural proteins associated with terminally differentiated myofibers. *rag2* and *cdh15* tumors expressed high levels of MRFs in the absence of terminal muscle differentiation, suggesting that overriding mechanisms in RMS cells block the capacity to undergo myogenesis.

Myogenin is an MRF that directs terminal differentiation of muscle progenitor cells (Pownall et al., 2002). Interestingly, a high proportion of *myogenin*-positive cells and overexpression of *myogenin* transcript are associated with poor prognosis in human (Blandford et al., 2006; Heerema-McKenney et al., 2008) and zebrafish RMS. Recent data have demonstrated a crucial role for *myogenin*-positive cells in the invasion and metastatic potential of RMS tumors (Ignatius et al., 2012). Our data further highlight the importance of *myogenin* as a prognostic marker and suggest that it is also a marker of aberrant regulation of the myogenic program in RMS. In *rag2* and *cdh15* tumors, *myogenin*-expressing cells, which make up the bulk of the tumor, fail to undergo terminal differentiation. In *mylz2* tumors, these *myogenin*-expressing cells do not accumulate but probably undergo differentiation. We propose that high *myogenin* expression, which is associated with poor survival in human RMS, might represent an inability of tumor cells to differentiate. Our data suggest that aberrant regulation of myogenesis is an important contributor to clinical outcome in RMS.

Gene expression analyses of RAS-induced zebrafish tumors highlight the ability of zebrafish tumors to model differing subtypes of human RMS. The gene signatures of the zebrafish tumors, although sharing a great deal of overlap, demonstrate that tumors driven by *mylz2* are more well differentiated than either *rag2* or *cdh15* tumors. Moreover, pathway analysis suggests that dysregulation of the PTEN tumor suppressor pathway may discern the *mylz2* from *rag2* tumors. This is consistent with studies showing

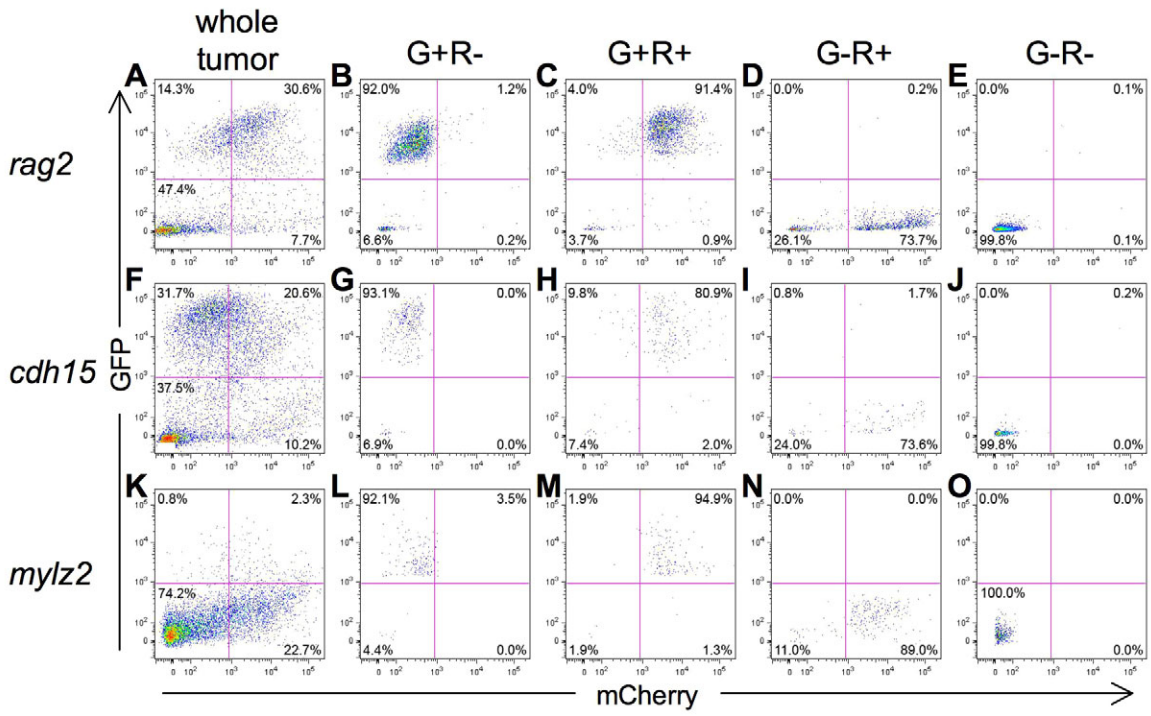

Fig. 7. Tumors in the *myf5:GFP;mylz2:mCherry* background have differing proportions of GFP- and mCherry-positive cells. (**A-O**) FACS profiles of a primary *rag2* (A), *cdh15* (F) and *mylz2* (K) tumor. G+R– (B,G,L), G+R+ (C,H,M), G–R+ (D,I,N) and G–R– (E,J,O) populations could be isolated with relative purity in *rag2* (B-E), *cdh15* (G-J) and *mylz2* (L-O) tumors.

that some human RMS might be sensitive to inhibition of downstream mTOR signaling with rapamycin (Hosoi et al., 1999). Subtypes of human RMS expressing PAX3 or PAX3-FKHR downregulate PTEN, allowing for continued tumor growth (Li et al., 2007). Several of the genes upregulated in the *rag2* and *cdh15* tumors, including *cyclin D1* and *fgfr4*, are known to interact with the PTEN pathway, and are involved in muscle differentiation. Cyclin D1 overexpression suppresses muscle differentiation in myoblasts by inhibiting the ability of MyoD to transactivate muscle-specific genes (Skapek et al., 1995) and might function similarly in RMS to block differentiation programs. Activating mutations in FGFR4 have recently been described in RMS, and FGFR4 is a transcriptional target of PAX3 and the PAX3-FKHR fusion protein (Lagha et al., 2008a; Taylor et al., 2009; Cao et al., 2010). FGF signaling has also been implicated in the maintenance of stem cell compartments in embryonic and adult muscle (Lagha et al., 2008b). Our data suggest that dysregulated FGF signaling contributes to RMS progression, perhaps through the activation of self-renewal pathways at the expense of differentiation programs, and that pathways required for normal muscle development and stem cell maintenance are utilized in tumors to mediate important aspects of tumor behavior.

Table 1. GFP-positive cells are enriched for tumor-propagating capability in *rag2*, *cdh15* and *mylz2* tumors

		Cells transplanted			
Tumor	Cell population	10,000	1000	100	10
rag2	G+R–	10/10	8/10	5/10	2/10
	G+R+	10/10	7/10	5/10	1/10
	G–R+	0/9	0/10	0/10	0/10
	G–R–	0/10	–	–	–
cdh15	G+R–	9/10	4/8	1/8	0/8
	G+R+	8/8	2/8	0/8	0/8
	G–R+	0/8	0/8	0/7	0/8
	G–R–	0/8	–	–	–
mylz2	G+R–	–	6/6	4/10	1/8
	G+R+	–	8/10	4/9	0/8
	G–R+	8/8	1/9	2/9	0/9
	G–R–	0/9	–	–	–

Results are depicted as number of fish showing tumor engraftment out of number of total fish transplanted for each dilution.

The role of cellular context in RMS formation

Prior studies have suggested that multiple cell types are capable of giving rise to RMS (Keller et al., 2004b; Keller et al., 2004a; Linardic et al., 2005; Langenau et al., 2007; Ren et al., 2008; Hettmer et al., 2011; Rubin et al., 2011; Hatley et al., 2012). In line with these studies, we have demonstrated that RMS formation can occur from the induction of oncogene expression at different times during myogenesis. The ability of tumors to recapitulate normal patterns of myogenesis differs considerably based on the timing of oncogene induction. Our data suggest that RAS activation in the context of differentiating muscle cells results in transformation but does not inhibit myogenic programs as it does in myoblasts. Similarly, ERMS tumors from the *Myf6* differentiating myoblast lineage in $p53^{-/-}$ mice show a higher degree of *in vitro* myogenic differentiation compared with tumors from the *Pax7* satellite cell lineage (Rubin et al., 2011). These data suggest that the differentiation capability of tumor cells reflects that of their respective cells of origin during development. Our data also raise the intriguing possibility that differences in clinical outcome can reflect differences in the tumor-initiating cell in RMS.

The *rag2* and *cdh15* tumors are highly similar despite differences in developmental expression patterns of these promoters. Transgene

expression in mosaic *rag2:KRAS^{G12D}* and *cdh15:KRAS^{G12D}* embryos is consistent with endogenous expression patterns, with significant *KRAS^{G12D}* expression seen in developing somites of *cdh15* but not *rag2* transgenics. In older larvae (5 dpf), *rag2* and *cdh15* promoter expression is undetectable within the trunk musculature of stable transgenics, consistent with endogenous expression (Fig. 1L; supplementary material Fig. S3H). In 5 dpf mosaic transgenics, *KRAS^{G12D}* transgene expression could be seen in a subset of muscle cells, possibly reflecting an expansion of muscle progenitor cells in larvae that go on to form tumors (supplementary material Fig. S4H,X,FF). In a rare (1 out of 71) 24 hpf *rag2:KRAS^{G12D}* embryo, an aggregate of transgene-positive cells could be seen (supplementary material Fig. S4O), suggesting an expansion of *KRAS^{G12D}*-expressing cells even at this early stage.

The tumor models described here do not show dramatic differences in global RAS expression or signaling within tumors. However, we cannot exclude the possibility that there are subpopulations of cells within tumors with very high or low levels of RAS expression that contribute to the differences in phenotypes that we have observed. It also remains unclear how RAS levels differ in the cells of origin at the time of transformation and how RAS expression may influence initial tumor formation and development. Because RAS levels are known to affect tumor phenotype in other models (Le et al., 2007), both cell of origin and RAS expression levels might contribute to the observed differences in tumor phenotype in our studies.

Recent experiments have demonstrated that *myf5*-expressing cells are highly enriched for tumor-propagating activity in *rag2* ERMS tumors (Ignatius et al., 2012). Here, we have shown that *myf5*-expressing cells are enriched for tumor-propagating activity in all zebrafish RMS tumor types. *myf5* expression, which is high in activated satellite cells and proliferating myoblasts, decreases during the course of muscle differentiation (Tomczak et al., 2004). Our data suggest that the most immature subpopulations within RMS tumors have the highest self-renewal capacity and also raise the interesting possibility that RMS cells behave according to a cellular hierarchy reminiscent of normal myogenesis, in which the most immature cells are capable of self-renewal and differentiation into cells that lack self-renewal and proliferative capacity.

Myf5 is a myogenic regulatory factor with important roles in muscle specification and regeneration (Rudnicki et al., 1993; Cooper et al., 1999; Ustanina et al., 2007). It is highly expressed in activated satellite cells and is upregulated in zebrafish, human and murine ERMS (Cornelison and Wold, 1997; Langenau et al., 2007; Zibat et al., 2010; Rubin et al., 2011). In *rag2* and *cdh15* tumors, *myf5*-expressing cells are abundant and have high self-renewal capability, reminiscent of activated satellite cells. In *mylz2* tumors, these cells are rare, express *myf5:GFP* at low levels, and display a strong propensity to undergo terminal differentiation. These observations suggest that satellite cell programs regulated by *myf5* may be reactivated in differentiating cell types that normally lack self-renewal and proliferative capacity, and that *myf5* might be an important driver of self-renewal in ERMS. *mylz2* tumors were the only tumors in which *myf5*-negative cells had discernible tumor-propagating activity. As these cells form the bulk of *mylz2* tumors, they represent a significant contributor to tumor growth in this model and suggest that self-renewal capability might remain active in more differentiated cell types in *mylz2* tumors. Taken together, our data suggest that the cellular context of the tumor-initiating cell during muscle development and pathways regulating normal muscle development may determine the self-renewal and differentiation programs used during RMS generation and growth.

In summary, we have demonstrated that induction of oncogenic RAS expression at different stages during muscle development has profound effects on the ability of tumor cells to recapitulate normal myogenesis, thus altering the tumorigenic capability of these cells. Our studies also suggest an important role for developmental pathways in mediating tumor behavior. Our zebrafish models will be useful reagents for elucidating the pathways that govern differentiation versus self-renewal and for understanding how cellular context can inform tumor behavior in RMS.

Acknowledgements
We thank Chuck Kaufman, Alison Taylor and Ginggi Storer for helpful discussions regarding this manuscript; Christian Lawrence, Isaac Adatto and Li-Kun Zhang for expert fish care; and Ellen Durand, Emily Huang, Ronald Mathieu and John Daley II for technical assistance.

Funding
This work was supported by the National Institutes of Health [R01CA103846 to L.I.Z.] and the National Institute of General Medical Sciences [T32GM007753 to N.Y.S.]. Deposited in PMC for release after 12 months.

Competing interests statement
The authors declare no competing financial interests.

Author contributions
N.Y.S., D.M.L. and L.I.Z. conceived the project and designed, analyzed and interpreted experiments. N.Y.S., R.M.W., and L.I.Z. wrote the manuscript with contributions from D.M.L. N.Y.S. performed the experiments. R.M.W. performed gene expression microarray analysis and gene set enrichment analysis. A.U. and E.P. provided technical assistance. G.P.N. assigned differentiation scores to histopathology slides.

Supplementary material
Supplementary material available online at
http://dev.biologists.org/lookup/suppl/doi:10.1242/dev.087858/-/DC1

References

Anderson, J., Gordon, A., Pritchard-Jones, K. and Shipley, J. (1999). Genes, chromosomes, and rhabdomyosarcoma. *Genes Chromosomes Cancer* **26**, 275-285.
Arndt, C. A. and Crist, W. M. (1999). Common musculoskeletal tumors of childhood and adolescence. *N. Engl. J. Med.* **341**, 342-352.
Barr, F. G. (1997). Molecular genetics and pathogenesis of rhabdomyosarcoma. *J. Pediatr. Hematol. Oncol.* **19**, 483-491.
Barr, F. G. (2001). Gene fusions involving PAX and FOX family members in alveolar rhabdomyosarcoma. *Oncogene* **20**, 5736-5746.
Blandford, M. C., Barr, F. G., Lynch, J. C., Randall, R. L., Qualman, S. J. and Keller, C. (2006). Rhabdomyosarcomas utilize developmental, myogenic growth factors for disease advantage: a report from the Children's Oncology Group. *Pediatr. Blood Cancer* **46**, 329-338.
Cao, L., Yu, Y., Bilke, S., Walker, R. L., Mayeenuddin, L. H., Azorsa, D. O., Yang, F., Pineda, M., Helman, L. J. and Meltzer, P. S. (2010). Genome-wide identification of PAX3-FKHR binding sites in rhabdomyosarcoma reveals candidate target genes important for development and cancer. *Cancer Res.* **70**, 6497-6508.
Chen, Y., Takita, J., Hiwatari, M., Igarashi, T., Hanada, R., Kikuchi, A., Hongo, T., Taki, T., Ogasawara, M., Shimada, A. et al. (2006). Mutations of the PTPN11 and RAS genes in rhabdomyosarcoma and pediatric hematological malignancies. *Genes Chromosomes Cancer* **45**, 583-591.
Chen, Y. H., Wang, Y. H., Chang, M. Y., Lin, C. Y., Weng, C. W., Westerfield, M. and Tsai, H. J. (2007). Multiple upstream modules regulate zebrafish myf5 expression. *BMC Dev. Biol.* **7**, 1.
Cooper, R. N., Tajbakhsh, S., Mouly, V., Cossu, G., Buckingham, M. and Butler-Browne, G. S. (1999). In vivo satellite cell activation via Myf5 and MyoD in regenerating mouse skeletal muscle. *J. Cell Sci.* **112**, 2895-2901.
Cornelison, D. D. and Wold, B. J. (1997). Single-cell analysis of regulatory gene expression in quiescent and activated mouse skeletal muscle satellite cells. *Dev. Biol.* **191**, 270-283.
Davicioni, E., Anderson, M. J., Finckenstein, F. G., Lynch, J. C., Qualman, S. J., Shimada, H., Schofield, D. E., Buckley, J. D., Meyer, W. H., Sorensen, P. H. et al. (2009). Molecular classification of rhabdomyosarcoma – genotypic and phenotypic determinants of diagnosis: a report from the Children's Oncology Group. *Am. J. Pathol.* **174**, 550-564.
Hatley, M. E., Tang, W., Garcia, M. R., Finkelstein, D., Millay, D. P., Liu, N., Graff, J., Galindo, R. L. and Olson, E. N. (2012). A mouse model of

rhabdomyosarcoma originating from the adipocyte lineage. *Cancer Cell* **22**, 536-546.
Heerema-McKenney, A., Wijnaendts, L. C., Pulliam, J. F., Lopez-Terrada, D., McKenney, J. K., Zhu, S., Montgomery, K., Mitchell, J., Marinelli, R. J., Hart, A. A. et al. (2008). Diffuse myogenin expression by immunohistochemistry is an independent marker of poor survival in pediatric rhabdomyosarcoma: a tissue microarray study of 71 primary tumors including correlation with molecular phenotype. *Am. J. Surg. Pathol.* **32**, 1513-1522.
Hettmer, S., Liu, J., Miller, C. M., Lindsay, M. C., Sparks, C. A., Guertin, D. A., Bronson, R. T., Langenau, D. M. and Wagers, A. J. (2011). Sarcomas induced in discrete subsets of prospectively isolated skeletal muscle cells. *Proc. Natl. Acad. Sci. USA* **108**, 20002-20007.
Hosoi, H., Dilling, M. B., Shikata, T., Liu, L. N., Shu, L., Ashmun, R. A., Germain, G. S., Abraham, R. T. and Houghton, P. J. (1999). Rapamycin causes poorly reversible inhibition of mTOR and induces p53-independent apoptosis in human rhabdomyosarcoma cells. *Cancer Res.* **59**, 886-894.
Ignatius, M. S., Chen, E., Elpek, N. M., Fuller, A. Z., Tenente, I. M., Clagg, R., Liu, S., Blackburn, J. S., Linardic, C. M., Rosenberg, A. E. et al. (2012). In vivo imaging of tumor-propagating cells, regional tumor heterogeneity, and dynamic cell movements in embryonal rhabdomyosarcoma. *Cancer Cell* **21**, 680-693.
Irintchev, A., Zeschnigk, M., Starzinski-Powitz, A. and Wernig, A. (1994). Expression pattern of M-cadherin in normal, denervated, and regenerating mouse muscles. *Dev. Dyn.* **199**, 326-337.
Keller, C., Hansen, M. S., Coffin, C. M. and Capecchi, M. R. (2004a). Pax3:Fkhr interferes with embryonic Pax3 and Pax7 function: implications for alveolar rhabdomyosarcoma cell of origin. *Genes Dev.* **18**, 2608-2613.
Keller, C., Arenkiel, B. R., Coffin, C. M., El-Bardeesy, N., DePinho, R. A. and Capecchi, M. R. (2004b). Alveolar rhabdomyosarcomas in conditional Pax3:Fkhr mice: cooperativity of Ink4a/ARF and Trp53 loss of function. *Genes Dev.* **18**, 2614-2626.
Lagha, M., Kormish, J. D., Rocancourt, D., Manceau, M., Epstein, J. A., Zaret, K. S., Relaix, F. and Buckingham, M. E. (2008a). Pax3 regulation of FGF signaling affects the progression of embryonic progenitor cells into the myogenic program. *Genes Dev.* **22**, 1828-1837.
Lagha, M., Sato, T., Bajard, L., Daubas, P., Esner, M., Montarras, D., Relaix, F. and Buckingham, M. (2008b). Regulation of skeletal muscle stem cell behavior by Pax3 and Pax7. *Cold Spring Harb. Symp. Quant. Biol.* **73**, 307-315.
Langenau, D. M., Traver, D., Ferrando, A. A., Kutok, J. L., Aster, J. C., Kanki, J. P., Lin, S., Prochownik, E., Trede, N. S., Zon, L. I. et al. (2003). Myc-induced T cell leukemia in transgenic zebrafish. *Science* **299**, 887-890.
Langenau, D. M., Keefe, M. D., Storer, N. Y., Guyon, J. R., Kutok, J. L., Le, X., Goessling, W., Neuberg, D. S., Kunkel, L. M. and Zon, L. I. (2007). Effects of RAS on the genesis of embryonal rhabdomyosarcoma. *Genes Dev.* **21**, 1382-1395.
Le, X., Langenau, D. M., Keefe, M. D., Kutok, J. L., Neuberg, D. S. and Zon, L. I. (2007). Heat shock-inducible Cre/Lox approaches to induce diverse types of tumors and hyperplasia in transgenic zebrafish. *Proc. Natl. Acad. Sci. USA* **104**, 9410-9415.
Li, H. G., Wang, Q., Li, H. M., Kumar, S., Parker, C., Slevin, M. and Kumar, P. (2007). PAX3 and PAX3-FKHR promote rhabdomyosarcoma cell survival through downregulation of PTEN. *Cancer Lett.* **253**, 215-223.
Linardic, C. M., Downie, D. L., Qualman, S., Bentley, R. C. and Counter, C. M. (2005). Genetic modeling of human rhabdomyosarcoma. *Cancer Res.* **65**, 4490-4495.
Livak, K. J. and Schmittgen, T. D. (2001). Analysis of relative gene expression data using real-time quantitative PCR and the 2(-Delta Delta C(T)) method. *Methods* **25**, 402-408.
Martinelli, S., McDowell, H. P., Vigne, S. D., Kokai, G., Uccini, S., Tartaglia, M. and Dominici, C. (2009). RAS signaling dysregulation in human embryonal Rhabdomyosarcoma. *Genes Chromosomes Cancer* **48**, 975-982.
Parker, M. H., Seale, P. and Rudnicki, M. A. (2003). Looking back to the embryo: defining transcriptional networks in adult myogenesis. *Nat. Rev. Genet.* **4**, 497-507.
Pownall, M. E., Gustafsson, M. K. and Emerson, C. P., Jr (2002). Myogenic regulatory factors and the specification of muscle progenitors in vertebrate embryos. *Annu. Rev. Cell Dev. Biol.* **18**, 747-783.
Ren, Y. X., Finckenstein, F. G., Abdueva, D. A., Shahbazian, V., Chung, B., Weinberg, K. I., Triche, T. J., Shimada, H. and Anderson, M. J. (2008). Mouse mesenchymal stem cells expressing PAX-FKHR form alveolar rhabdomyosarcomas by cooperating with secondary mutations. *Cancer Res.* **68**, 6587-6597.
Rubin, B. P., Nishijo, K., Chen, H. I., Yi, X., Schuetze, D. P., Pal, R., Prajapati, S. I., Abraham, J., Arenkiel, B. R., Chen, Q. R. et al. (2011). Evidence for an unanticipated relationship between undifferentiated pleomorphic sarcoma and embryonal rhabdomyosarcoma. *Cancer Cell* **19**, 177-191.
Rudnicki, M. A., Schnegelsberg, P. N., Stead, R. H., Braun, T., Arnold, H. H. and Jaenisch, R. (1993). MyoD or Myf-5 is required for the formation of skeletal muscle. *Cell* **75**, 1351-1359.
Skapek, S. X., Rhee, J., Spicer, D. B. and Lassar, A. B. (1995). Inhibition of myogenic differentiation in proliferating myoblasts by cyclin D1-dependent kinase. *Science* **267**, 1022-1024.
Smith, A. C., Raimondi, A. R., Salthouse, C. D., Ignatius, M. S., Blackburn, J. S., Mizgirev, I. V., Storer, N. Y., de Jong, J. L., Chen, A. T., Zhou, Y. et al. (2010). High-throughput cell transplantation establishes that tumor-initiating cells are abundant in zebrafish T-cell acute lymphoblastic leukemia. *Blood* **115**, 3296-3303.
Stratton, M. R., Fisher, C., Gusterson, B. A. and Cooper, C. S. (1989). Detection of point mutations in N-ras and K-ras genes of human embryonal rhabdomyosarcomas using oligonucleotide probes and the polymerase chain reaction. *Cancer Res.* **49**, 6324-6327.
Taylor, J. G., 6th, Cheuk, A. T., Tsang, P. S., Chung, J. Y., Song, Y. K., Desai, K., Yu, Y., Chen, Q. R., Shah, K., Youngblood, V. et al. (2009). Identification of FGFR4-activating mutations in human rhabdomyosarcomas that promote metastasis in xenotransplanted models. *J. Clin. Invest.* **119**, 3395-3407.
Thisse, C., Thisse, B., Schilling, T. F. and Postlethwait, J. H. (1993). Structure of the zebrafish snail1 gene and its expression in wild-type, spadetail and no tail mutant embryos. *Development* **119**, 1203-1215.
Tomczak, K. K., Marinescu, V. D., Ramoni, M. F., Sanoudou, D., Montanaro, F., Han, M., Kunkel, L. M., Kohane, I. S. and Beggs, A. H. (2004). Expression profiling and identification of novel genes involved in myogenic differentiation. *FASEB J.* **18**, 403-405.
Traver, D., Paw, B. H., Poss, K. D., Penberthy, W. T., Lin, S. and Zon, L. I. (2003). Transplantation and in vivo imaging of multilineage engraftment in zebrafish bloodless mutants. *Nat. Immunol.* **4**, 1238-1246.
Ustanina, S., Carvajal, J., Rigby, P. and Braun, T. (2007). The myogenic factor Myf5 supports efficient skeletal muscle regeneration by enabling transient myoblast amplification. *Stem Cells* **25**, 2006-2016.
Westerfield, M. (1989). *The Zebrafish Book: A Guide For The Laboratory Use of Zebrafish.* Eugene, OR: University of Oregon Press.
Wexler, L. H. and Helman, L. J. (1994). Pediatric soft tissue sarcomas. *CA Cancer J. Clin.* **44**, 211-247.
White, R. M., Sessa, A., Burke, C., Bowman, T., LeBlanc, J., Ceol, C., Bourque, C., Dovey, M., Goessling, W., Burns, C. E. et al. (2008). Transparent adult zebrafish as a tool for in vivo transplantation analysis. *Cell Stem Cell* **2**, 183-189.
Xu, Y., He, J., Wang, X., Lim, T. M. and Gong, Z. (2000). Asynchronous activation of 10 muscle-specific protein (MSP) genes during zebrafish somitogenesis. *Dev. Dyn.* **219**, 201-215.
Zeschnigk, M., Kozian, D., Kuch, C., Schmoll, M. and Starzinski-Powitz, A. (1995). Involvement of M-cadherin in terminal differentiation of skeletal muscle cells. *J. Cell Sci.* **108**, 2973-2981.
Zibat, A., Missiaglia, E., Rosenberger, A., Pritchard-Jones, K., Shipley, J., Hahn, H. and Fulda, S. (2010). Activation of the hedgehog pathway confers a poor prognosis in embryonal and fusion gene-negative alveolar rhabdomyosarcoma. *Oncogene* **29**, 6323-6330.